DIFFRACTIVE DISSOCIATION IN HIGH ENERGY pp COLLISIONS IN ADDITIVE QUARK MODEL

Yu.M. Shabelski and A.G. Shuvaev

Petersburg Nuclear Physics Institute, Kurchatov National Research Center
Gatchina, St. Petersburg 188300, Russia

E-mail: shabelsk@thd.pnpi.spb.ru
E-mail: shuvaev@thd.pnpi.spb.ru

Abstract

High energy (CERN SPS and LHC) pp ($p\bar{p}$) scattering is treated in the framework of Additive Quark Model together with Pomeron exchange theory. The reasonable agreement with experimental data is achieved both for the elastic scattering and for the diffractive dissociation with natural parameters for the strong matter distribution inside proton.

PACS. 25.75.Dw Particle and resonance production

1 Introduction

Regge theory provides a useful tool for phenomenological description of high energy hadron collisions [1, 2, 3, 4]. The quantitative predictions of Regge calculus are essentially dependent on the assumed coupling of participating hadrons to Pomeron. In our previous paper [5] we described elastic pp ($p\bar{p}$) scattering including the recent LHC data in terms of simple Regge exchange approach in the framework of Additive Quark Model (AQM) [6, 7]. In the present paper we extend our description to the processes of single and double diffractive dissociation.

In AQM baryon is treated as a system of three spatially separated compact objects – constituent quarks. Each constituent quark is colored, has internal quark-gluon structure and finite radius that is much less than the radius of proton, $r_q^2 \ll r_p^2$. This picture is in good agreement both with $SU(3)$ symmetry of strong interaction and the

quark-gluon structure of proton [8, 9]. The constituent quarks play the roles of incident particles in terms of which pp scattering is described in AQM.

To make the main ingredients and notations of our approach more clear we start from the elastic scattering in the section 2. The formalism used to describe single and double diffractive dissociation is presented in the section 3 while the obtained numerical results are compared with the experimental data in the section 4.

2 Elastic Scattering Amplitude in AQM

Elastic amplitudes for the large energy $s = (p_1 + p_2)^2$ and small momentum transfer t are dominated by the Pomeron exchange. We neglect the small difference in pp and $p\bar{p}$ scattering coming from the exchange of negative signature Reggeons, Odderon (see e.g. [10] and references therein), ω-Reggeon etc, since their contribution is suppressed by s.

The single t-channel exchange results into amplitude of constituent quarks scattering

$$M_{qq}^{(1)}(s,t) = \gamma_{qq}(t) \cdot \left(\frac{s}{s_0}\right)^{\alpha_P(t)-1} \cdot \eta_P(t) \ , \tag{1}$$

where $\alpha_P(t) = \alpha_P(0) + \alpha'_P \cdot t$ is the Pomeron trajectory specified by the intercept, $\alpha_P(0)$, and slope, α'_P, values. The Pomeron signature factor,

$$\eta_P(t) \ = \ i \ - \ \tan^{-1}\left(\frac{\pi\alpha_P(t)}{2}\right),$$

determines the complex structure of the amplitude. The factor $\gamma_{qq}(t) = g_1(t) \cdot g_2(t)$ has the meaning of the Pomeron coupling to the beam and target particles, the functions $g_{1,2}(t)$ being the vertices of constituent quark-Pomeron interaction (filled circles in Fig. 1).

Due to factorization of longitudinal and transverse degrees of freedom the longitudinal momenta are integrated over separately in high energy limit. After this the transverse part of the quark distribution is actually relevant only. It is described by the wavefunction $\psi(k_1, k_2, k_3)$, where k_i are the quark transverse momenta, normalized as

$$\int dK \, |\psi(k_1, k_2, k_3)|^2 \ = \ 1, \tag{2}$$

and a shorthand notation is used

$$dK \ \equiv \ d^2k_1 d^2k_2 d^2k_3 \, \delta^{(2)}(k_1 + k_2 + k_3).$$

The elastic pp (or $p\bar{p}$, here we do not distinguish between them) scattering amplitude is basically expressed in terms of the wavefunction as

$$M_{pp}(s,t) \;=\; \int dK\, dK' \psi^*(k_i'+Q_i')\, \psi^*(k_i+Q_i)\, V(Q,Q')\, \psi(k_i')\, \psi(k_i). \qquad (3)$$

In this formula $\psi(k_i) \equiv \psi(k_1,k_2,k_3)$, is the initial proton wavefunction $\psi(k_i+Q_i) \equiv \psi(k_1+Q_1,k_2+Q_2,k_3+Q_3)$ is the wavefunction of the scattered proton, and the interaction vertex $V(Q,Q') \equiv V(Q_1,Q_2,Q_3,Q_1',Q_2',Q_3')$ stands for the multipomeron exchange, Q_k and Q_l' are the momenta transferred to the target quark k or beam quark l by the Pomerons attached to them, Q is the total momentum transferred in the scattering, $Q^2=-t$.

The scattering amplitude is presented in AQM as a sum over the terms with a given number of Pomerons,

$$M_{pp}(s,t) \;=\; \sum_n M_{pp}^{(n)}(s,t), \qquad (4)$$

where the amplitudes $M_{pp}^{(n)}$ collect all diagrams comprising various connections of the beam and target quark lines with n Pomerons.

Similar to Glauber theory [11, 12] one has to rule out the multiple interactions between the same quark pair. AQM permits the Pomeron to connect any two quark lines only once. It crucially decreases the combinatorics leaving the diagrams with no more than $n=9$ effective Pomerons. Several AQM diagrams are shown in Fig. 1.

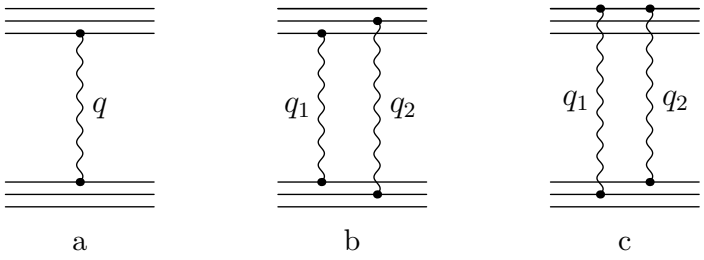

Figure 1: The AQM diagrams for pp elastic scattering. The straight lines stand for quarks, the waved lines denote Pomerons, Q is the momentum transferred, $t=-Q^2$. Diagram (a) is the one of the single Pomeron diagrams, diagrams (b) and (c) represent double Pomeron exchange with two Pomeron coupled to the different quark (b) and to the same quarks (c), $q_1+q_2=Q$.

In what follows we assume the Pomeron trajectory in the simplest form

$$\left(\frac{s}{s_0}\right)^{\alpha_P(t)-1} \;=\; e^{\Delta\cdot\xi} e^{-r_q^2 q^2}, \quad \xi \equiv \ln\frac{s}{s_0}, \quad r_q^2 \equiv \alpha'\cdot\xi.$$

The value r_q^2 defines the radius of quark-quark interaction while $S_0 = (9\ \mathrm{GeV})^2$ has the meaning of typical energy scale in Regge theory.

In the first order there are 9 equal quark-quark contributions due to one Pomeron exchange between qq pairs. The amplitude (3) reduces to a single term with $Q_1 = Q_1' = Q$, $Q_{2,3} = Q_{2,3}' = 0$,

$$M_{pp}^{(1)} \ = \ 9\Big(\gamma_{qq}\eta_P(t)e^{\Delta\cdot\xi}\Big)\, e^{-r_q^2\, Q^2} F_P(Q,0,0)^2, \tag{5}$$

expressed through the overlap function

$$F_P(Q_1,Q_2,Q_3) \ = \ \int dK\, \psi^*(k_1,k_2,k_3)\, \psi(k_1+Q_1,k_2+Q_2,k_3+Q_3). \tag{6}$$

The function $F_P(Q,0,0)$ plays a role of proton formfactor for the strong interaction in AQM.

An example of the second order diagrams is shown in Fig. 1b,c. Denoting $q_{1,2}$ the transverse momenta carried by the Pomerons, we have for the diagram b $Q_1 = Q_3' = 0$, $Q_2 = Q_2' = q_2$, $Q_3 = Q_1' = q_1$ and for the diagram c $Q_1 = q_1 + q_2$, $Q_2 = Q_3 = 0$, $Q_2' = q_1$, $Q_3' = 0$.

Generally, the higher orders elastic terms are expressed through the functions (6) integrated over Pomerons' momenta,

$$\begin{aligned} M^{(n)}(s,t) \ &= \ i^{n-1}\Big(\gamma_{qq}\eta_P(t_n)e^{\Delta\cdot\xi}\Big)^n \int \frac{d^2q_1}{\pi}\cdots\frac{d^2q_n}{\pi}\,\pi\,\delta^{(2)}(q_1+\ldots+\,q_n-Q) \qquad (7)\\ &\quad \times e^{-r_q^2(q_1^2+\ldots+q_n^2)}\,\frac{1}{n!}\sum_{n\ \text{connections}} F_P(Q_1,Q_2,Q_3)\,F_P(Q_1',Q_2',Q_3'), \quad t_n \simeq t/n. \end{aligned}$$

The sum in this formula refers to all distinct ways to connect the beam and target quark lines with n Pomerons in the scattering diagram. The set of momenta Q_i and Q_l' the quarks acquire from the attached Pomerons is particular for each connection pattern. More detailed description can be found in [5].

With the amplitude (4) the differential cross section in the normalization adopted here is evaluated as

$$\frac{d\sigma}{dt} \ = \ 4\pi\,|M_{pp}(s,t)|^2. \tag{8}$$

The optical theorem, that relates the total elastic cross section and imaginary part of the amplitude, in this normalization reads

$$\sigma_{pp}^{tot} \ = \ 8\pi\,\mathrm{Im}\,M_{pp}(s,t=0).$$

Recall once more that exchanges of the positive signature Reggeons determine, strictly speaking, half of the sum of pp and $p\bar{p}$ elastic amplitude. Their difference is neglected in the present approach.

3 Cross section of single and double diffractive dissociation

The Glauber theory makes it possible to find as well the cross sections of excitation or disintegration of one or both colliding objects. The close approximation (completness condition) ([12, 13] allows one to calculate the total cross sections of all processes related to the elastic scattering of constituents but without giving rise to new particles production,

$$\frac{d\sigma}{dt}(pp \to p'p') = \frac{d\sigma}{dt}(pp \to pp) + 2\frac{d\sigma}{dt}(pp \to p^*p) + \frac{d\sigma}{dt}(pp \to p^*p^*)$$

Here $d\sigma(pp \to pp)/dt = d\sigma_{el}/dt$ is the elastic pp scattering cross section shown in Fig. 2a. The situations when one scattered constituent receives comparatively large

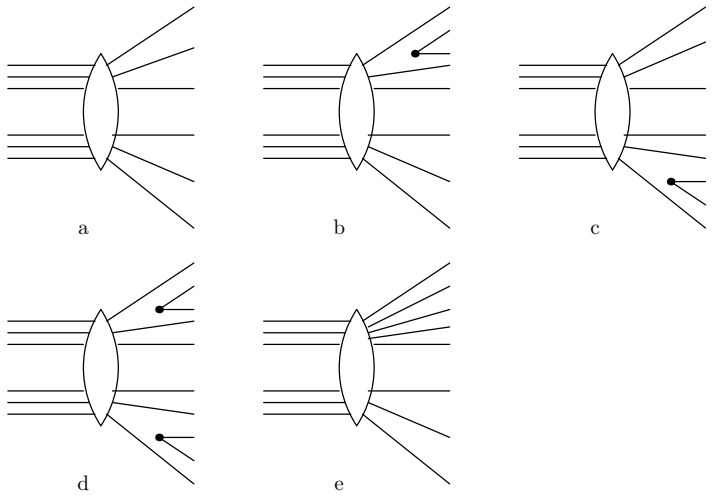

Figure 2: Different final states in the high energy pp collision: a) elastic pp scattering, b) and c) single diffractive dissociation of first or second proton, d) double diffractive dissociation, e) process with one $q\bar{q}$ pair inelastic production that does not contribute to the calculated σ_{SD} but can contribute to the experimental value σ_{SD}.

transverse momentum is shown in Fig. 2b and Fig. 2c. In the case of nucleus-nucleus collision it results in the excitation or disintegration of one of the nucleus. In the case

of pp collisions in AQM a scattered quark moves far away from the remnant at the distance ~ 1 fm where a new $q\bar{q}$ pair is produced due to quark confinement effects. It can be interpreted as a diffractive production of a single jets, $\sigma(pp \to pp^*) = \sigma_{SD}$, say, one or several pions, $p \to p + n \times \pi$. Similarly two diffractive jet are produced in the case of Fig 2d, $\sigma(pp \to p^*p^*) = \sigma_{DD}$. In Fig 2e a new $q\bar{q}$ pair is produced as a part of multipheral ladder independently of the quarks wavefunction leaving it essentially intact. This process is related to the inelastic interaction of the constituents and does not contribute to $d\sigma(p'p')/dt$ in AQM.

The amplitude of single diffraction dissociation reads

$$M_{SD}(s,t) \;=\; \int dK\, dK' \psi^*(k_i' + Q')\, \widetilde{\psi}^*_m(k_i + Q_i)\, V(Q,Q')\, \psi(k_i')\, \psi(k_i). \tag{9}$$

Here the wavefunction of one of the protons remains unchanged whereas the other proton turns into p^* final state specified with the wavefunction $\widetilde{\psi}_m(k_i)$.

The double diffraction dissociation implies both protons to be in the p^* final states,

$$M_{DD}(s,t) \;=\; \int dK\, dK' \widetilde{\psi}^*_m(k_i' + Q')\, \widetilde{\psi}^*_n(k_i + Q_i)\, V(Q,Q')\, \psi(k_i')\, \psi(k_i). \tag{10}$$

To obtain cross section one has to square the module of an appropriate amplitude. Making no distinction between the individual final states it should be summed up over m for (9) process or over m and n indices for (10) process. For DD case it gives

$$\begin{aligned} &\frac{d\sigma_{el}}{dt} \;+\; 2\,\frac{d\sigma_{SD}}{dt} \;+\; \frac{d\sigma_{DD}}{dt} \\ =\;& 4\pi \sum_{m,n} \int dK\, dK'\, dP\, dP'\, \widetilde{\psi}^*_m(k_i' + Q_i')\, \widetilde{\psi}^*_m(k_i + Q_i)\, V(Q,Q') \psi(k_i')\, \psi(k_i) \\ &\times \psi^*(p_i)\psi^*(p_i')\; V^*(Q'',Q''') \widetilde{\psi}_m(p_i' + Q_i''') \widetilde{\psi}_n(p_i + Q_i'') \end{aligned} \tag{11}$$

Using now the completeness condition,

$$\sum_n \widetilde{\psi}_n(p_i + Q_i'')\, \widetilde{\psi}^*_n(k_i + Q_i) \;=\; \delta^{(2)}(p_i + Q_i'' - k_i - Q_i)$$

along with the same condition for the index m we get

$$\begin{aligned} &\frac{d\sigma_{el}}{dt} \;+\; 2\,\frac{d\sigma_{SD}}{dt} \;+\; \frac{d\sigma_{DD}}{dt} \\ =\;& \int dK\, dK' \psi^*(k_i + Q_i - Q_i''') \psi^*(k_i' + Q_i' - Q_i'')\, V(Q,Q') V^*(Q'',Q''') \psi(k_i') \psi(k_i). \end{aligned} \tag{12}$$

The double diffractive dissociation cross section is provided by the two sets of the Pomeron exchange diagrams separately associated with the "left" interaction vertex

$V(Q,Q')$ and the "right" one $V^*(Q'',Q''')$. They are summed up independently over the total numbers of the Pomerons participating in the diagram "from the left" or "from the right", $m,n=1,9$,

$$\frac{d\sigma_{el}}{dt} \,+\, 2\,\frac{d\sigma_{SD}}{dt} \,+\, \frac{d\sigma_{DD}}{dt} \,=\, \sum_{m,n} |M^{(m,n)}_{p'p'}|^2(s,t).$$

Substituting here the Pomeron-quark vertex and introduced above overlap function (6), we express each term in the sum as

$$\begin{aligned}
|M^{(m,n)}_{p'p'}|^2 \,&=\, \left(\gamma_{qq}e^{\Delta\cdot\xi}\right)^{m+n} [\,i\eta_P(t_m)]^m\,[-i\eta^*_P(t_n)]^n \qquad (13)\\
&\times \int \frac{d^2q_1}{\pi}\cdots\frac{d^2q_m}{\pi}\,\pi\,\delta^{(2)}(q_1+\ldots+\,q_m-Q)\\
&\times \frac{d^2q_{m+1}}{\pi}\cdots\frac{d^2q_{m+n}}{\pi}\,\pi\,\delta^{(2)}(q_{m+1}+\ldots+\,q_{m+n}-Q)\\
&\times e^{-r_q^2(q_1^2+\ldots+q^2_{m+n})}\,\frac{1}{m!}\,\frac{1}{n!}\sum_{m,n\ \text{connections}} F_P(Q_1,Q_2,Q_3)\,F_P(Q'_1,Q'_2,Q'_3).
\end{aligned}$$

For the single diffractive dissociation the cross section includes the single sum over the final states of one of the protons. In this case the completeness condition gives

$$\frac{d\sigma_{SD}}{dt} \,+\, \frac{d\sigma_{el}}{dt} \,=\, 4\pi\sum_{m,n} |M^{(m,n)}_{pp'}|^2(s,t),$$

with

$$\begin{aligned}
|M^{(m,n)}_{pp'}|^2 \,&=\, \left(\gamma_{qq}e^{\Delta\cdot\xi}\right)^{m+n} [\,i\eta_P(t_m)]^m\,[-i\eta^*_P(t_n)]^n \qquad (14)\\
&\times \int \frac{d^2q_1}{\pi}\cdots\frac{d^2q_m}{\pi}\,\pi\,\delta^{(2)}(q_1+\ldots+\,q_m-Q)\\
&\times \frac{d^2q_{m+1}}{\pi}\cdots\frac{d^2q_{m+n}}{\pi}\,\pi\,\delta^{(2)}(q_{m+1}+\ldots+\,q_{m+n}-Q)\,e^{-r_q^2(q_1^2+\ldots+q^2_{m+n})}\\
&\times \frac{1}{m!}\frac{1}{n!}\sum_{m,n\ \text{connections}} F_P(Q_1,Q_2,Q_3)\,F_P(Q'_1,Q'_2,Q'_3)\;F_P(Q''_1,Q''_2,Q''_3)
\end{aligned}$$

The first function F_P appears here from the completeness condition written for the dissociating proton while two other F_P functions in the product stand for elastically scattered proton.

4 Numerical calculations

The expressions (13,14) have been used for the numerical calculation of the single and double diffractive dissociation of the protons together with the formula (7) for their elastic scattering. The overlap function (6) is evaluated through the transverse part of the quarks' wavefunction, which has been taken in a simple form of two gaussian packets,

$$\psi(k_1,k_2,k_3) \;=\; N[\,e^{-a_1(k_1^2+k_2^2+k_3^2)} \;+\; C\,e^{-a_2(k_1^2+k_2^2+k_3^2)}], \tag{15}$$

normalized to unity (2). One packet parametrization, $C = 0$, is insufficient to reproduce the experimental data on elastic scattering [5] as imposing too strong mutual dependence between the total cross section, the minimum position in $d\sigma_{el}/dt$ and the value of the slope at $t = 0$.

All parameters used in the calculation naturally fall into two different kinds: the parameters of the Pomeron and those specifying the structure of colliding particles. The former type, Δ, α', γ_{qq}, refers to the high energy scattering theory while the latter, $a_{1,2}$ and C, details the matter distribution inside the proton in the low energy limit(similar to density distribution in atomic nuclear).

We recalculate the elastic scattering cross section $d\sigma_{el}/dt$, obtained in our previous paper [5] assuming the argument of the signature factor $t_n = t/n = -Q^2/n$ that is natural for Gaussian Q^2 dependence. It causes a slight change of the model parameters. Now the Pomeron parameters are

$$\Delta = 0.107, \quad \alpha' = 0.31\,\mathrm{GeV}^{-2}, \quad \gamma_{qq} = 0.44\,\mathrm{GeV}^{-2},$$

and the parameters of matter distribution in the proton are

$$a_1 = 4.8\,\mathrm{GeV}^{-2}, \quad a_2 = 1.02\,\mathrm{GeV}^{-2}, \quad C = 0.133.$$

Note that the same set of the Pomeron parameters describes proton and antiproton scattering, therefore both pp and $p\bar{p}$ data have been commonly used to fix their values.

The model gives a reasonable description of elastic scattering experimental data both for pp collisions at $\sqrt{s} = 7$ TeV and $p\bar{p}$ collisions at $\sqrt{s} = 546$ GeV, see Fig. 3. The obtained curves only are slightly different from those published in the previous paper [5].

The results for the SD and DD cross sections are presented in the Table 1. The SD cross sections come out to be rather small, $\sigma_{SD}/\sigma_{el} \simeq 15 - 18\%$, that matches perhaps the experimental results at LHC energies [18, 19, 20]. The total diffraction cross section is approximately half the elastic one, $2\sigma_{SD} + \sigma_{DD} \simeq \sigma_{el}/2$, within the range of available energy dependence of the probability of diffractive to elastic scattering.

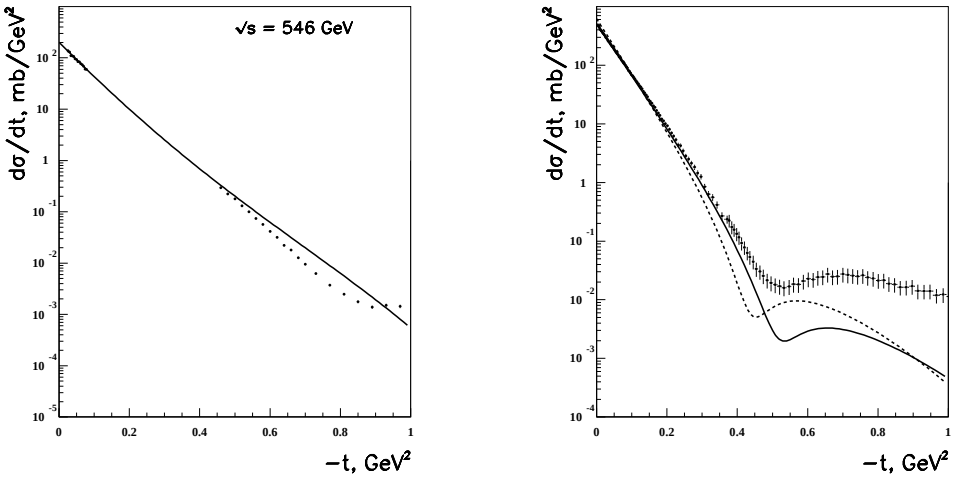

Figure 3: The differential cross section of elastic $p\bar{p}$ scattering at $\sqrt{s} = 546$ GeV (left panel) and for the elastic pp collisions at $\sqrt{s} = 7$ TeV (right panel, solid line) compared to the experimental data. The dotted line at the right panel shows the predicted elastic pp cross section at $\sqrt{s} = 13$ TeV. The experimental points have been taken from [14, 15, 16, 17].

The ratio σ_{SD}/σ_{el} is in somewhat inconsistency ($1.5 \div 2$ times lesser) with the intermediate energy estimation in [21]. We get $\sigma_{SD} \approx \sigma_{DD}$, so that σ_{DD}/σ_{el} is not quadratically small compared to σ_{SD}/σ_{el}. The reason for this comes in AQM from an extra third formfactor F_P in the SD cross section (14) compared to the two formfactors in the DD formula (13). On the other hand the connection between diffractive cross section calculated in AQM and the experimental data is not straightforward since AQM comprises only a part of the processes involved in the scattering. The processes shown in Fig. 2e are not accounted for in AQM although their contribution to the experimentally measured σ_{SD} is quite possible.

Table 1.

$\sqrt{s}$	σ_{el} (mb)	$\sigma_{SD}(mb)$	$\sigma_{DD}(mb)$
546 GeV	14.3	2.3	2.6
7 TeV	27.3	4.3	3.9
13 TeV	31.6	5.4	4.9

Motivated by the recently announced new LHC run we present also the predictions for the elastic pp scattering and diffractive dissociation at $\sqrt{s} = 13$ TeV. In particular, we expect the total cross section $\sigma(pp)_{tot} = 110$ mb, the parameter of the elastic slope cone $B = 21.8$, the minimum position at $|t| = 0.45$ GeV^2 while our results for the differential cross section, $d\sigma_{el}/dt$, are shown in Fig. 3.

Fig. 4 shows our results for the differential cross sections $d\sigma_{SD}/dt$ and $d\sigma_{DD}/dt$ at $\sqrt{s} = 546$ GeV. Unfortunately we are unable to predict at small $|t| < 0.1$ Gev^2 because

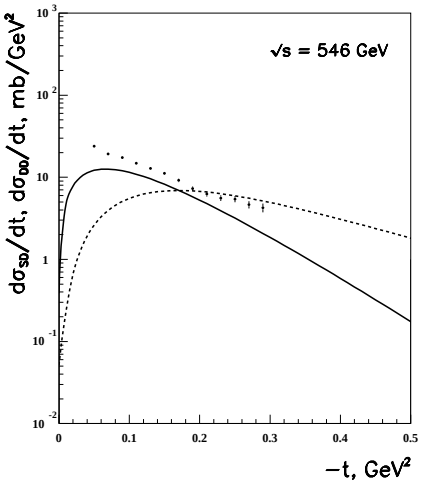

Figure 4: The cross section of single (solid line) and double (dotted line) diffractive dissociation in $p\bar{p}$ scattering at $\sqrt{s} = 546$ GeV. The experimental SD points have been taken from [22].

of the unknown effects of confinement that could lead to the transition between the ground and excited states. However such a transition can not change the total cross sections (13), (14) calculated with the help of the close approximation. The region $|t| > 1$ Gev^2 is beyond the reach of our model as well since the internal structure of the constituent quarks can not be more ignored there. The diffractive cross section behavior in the intermediate interval is in reasonable agreement with the experimental data.

5 Conclusion

We have presented the unified description of the elastic and diffractive pp ($p\bar{p}$) scattering in the framework of AQM. The main feature of our model is a common set of parameters it employs. After fitting the parameters that describe the elastic scattering no more ones have been added for the diffractive case. The parameters chosen are mainly determined by the structure of the quark wavefunction for the initial state. Despite this the model yields reasonable calculated values both for the SD and DD cross sections that can be recognized as a one further argument in favor of AQM applicability for the high energy pp scattering.

The authors are grateful to M.G. Ryskin for helpful discussion.

References

[1] I. M. Dremin, Phys. Usp. **56** (2013) 3 [Usp. Fiz. Nauk **183** (2013) 3] [arXiv:1206.5474 [hep-ph]].

[2] M. G. Ryskin, A. D. Martin and V. A. Khoze, Eur. Phys. J. C **72** (2012) 1937

[3] C. Merino and Y. .M. Shabelski, JHEP **1205** (2012) 013 [arXiv:1204.0769 [hep-ph]].

[4] O. V. Selyugin, Eur. Phys. J. C **72** (2012) 2073 [arXiv:1201.4458 [hep-ph]].

[5] Y. M. Shabelski and A. G. Shuvaev, JHEP **1411** (2014) 023 [arXiv:1406.1421 [hep-ph]].

[6] E. M. Levin and L. L. Frankfurt, JETP Lett. **2** (1965) 65.

[7] J. J. J. Kokkedee and L. Van Hove, Nuovo Cim. **42** (1966) 711.

[8] Y. L. Dokshitzer, D. Diakonov and S. I. Troian, Phys. Rept. **58**, 269 (1980).

[9] V. M. Shekhter, Yad.Fiz. **33** (1981) 817; Sov. J. Nucl. Phys. **33** (1981) 426.

[10] R. Avila, P. Gauron and B. Nicolescu, Eur. Phys. J. C **49**, 581 (2007) [hep-ph/0607089].

[11] R. J. Glauber. In "Lectures in Theoretical Physics", Eds. W. E. Brittin etal., New York (1959), vol.1, p.315.

[12] V. Franco and R. J. Glauber, Phys.Rev. **142** (1966) 1195.

[13] V. M. Braun and Y. M. Shabelski, Sov. J. Nucl. Phys. **35** (1982) 731 [Yad. Fiz. **35**(1982) 1247].

[14] F. Abe *et al.* [CDF Collaboration], Phys. Rev. D **50** (1994) 5518.

[15] G. Antchev et al., TOTEM Collaboration, Europhys. Lett. **96**, 21002 (2011).

[16] TOTEM Collaboration, G. Antchev et al., Europhys.Lett. **101** (2013) 21002.

[17] TOTEM Collaboration, G. Antchev et al., Europhys.Lett. **95** (2011) 41001, [arXiv:1110.1385].

[18] G. Antchev *et al.* [TOTEM Collaboration], Europhys. Lett. **101** (2013) 21003.

[19] TOTEM coll. F. Oljemark and K. Osterberg "Studies of soft single diffraction with TOTEM at $\sqrt{s} = 7$ TeV" LHC students poster session, 13 March 2013.

[20] V. A. Khoze, A. D. Martin and M. G. Ryskin, Int. J. Mod. Phys. A **30** (2015) 08, 1542004, [arXiv:1402.2778 [hep-ph]].

[21] A. B. Kaidalov, Phys. Rept. **50** (1979) 157.

[22] D. Bernard *et al.* [UA4 Collaboration], Phys. Lett. B **186** (1987) 227.